Grenze International Journal of Engineering and Technology, Jan Issue

An Image Mining Approach to Classify Dental Images into Normal and Caries-Infected using a Reduced Textural Feature Set

Prerna Singh[1], Priti Sehgal[2] and Roli Bansal[3]
[1]Department of Computer Science, University of Delhi, Delhi. India
Email: prerna.singh@jimsindia.org
[2-3]Department of Computer Science, Keshav Mahavidyalaya, University of Delhi, Delhi, India
Email:{psehgal, roli.bansal}@hostname2.org

***Abstract*—Image mining is an emerging research field in the digital era. Medical image mining is critical and challenging as medical images contain vital information for characterizing health disorders. Research studies on dental images using data mining classification techniques have revealed infected tooth issues, enabling an accurate automatic interpretation of diseases in clinical imaging. In this study, we present an image mining approach that uses a reduced feature set to classify dental images as normal and caries-infected. Our approach first extracts features from dental images using four feature extraction methods: Local Binary Pattern (LBP), Gray Level Co-occurrence Matrix (GLCM), Gray Level Run Length Matrix (GLRLM) and Local Binary Gray Level Co-occurrence Matrix (LBGLCM). The obtained feature sets are reduced using principal component analysis and then each respective reduced set is subjected to various classification techniques to identify the normal and caries infected dental images. The AdaBoost classifier with the reduced feature set obtained by LBGLCM, GLCM and LBP methods achieved the highest accuracy of 99.7%, 98.7% and 90.8% respectively, whereas the multilayer perceptron layer classifier with the reduced feature set obtained by GLRLM method achieved the best accuracy of 97.9%, demonstrating the efficacy of our reduced textural feature set based approach for dental image classification.**

***Index Terms*— image mining, dental images classification, infected tooth, AdaBoost, multilayer perceptron.**

I. INTRODUCTION

In image mining, large amounts of available image data are analyzed to discover new and important information. Advances in image acquisition and storage have resulted in generating a large number of images in all disciplines of life including medicine. These medical images can be effectively used as the starting/fundamental material to study various disease pathologies. Medical image mining plays a critical role in healthcare informatics. It attempts to identify significant patterns in a given set of such images which could prove beneficial for the diagnosis of various pathological conditions.

The treatment of dental caries is dependent on its timely detection and diagnosis. As dental caries is a bacterial transmissible disease, it can spread to the adjacent teeth and cause teech destruction. The diagnosis and treatment of dental caries are primarily based on radiographs/X-rays. This motivated us to apply image mining

Grenze ID: 01.GIJET.9.1.538_1

techniques to dental im- ages for detecting tooth abnormalities and diseases.

This paper presents a novel reduced textural feature-based approach for classifying dental images as normal or caries-infected. The features are first collected using some state-of-the-art textural feature extraction methods. The extracted features are then subjected to Principal Component Analysis (PCA) for reduction. Finally, the reduced features are used for the desired classification.

The remainder of this paper is organized as follows. Section 2 discusses various studies that have investigated/employed image mining for dental images. Section 3 presents the proposed technique, while Section 4 discusses the experimental results. Finally, section 5 presents the conclusions and future work.

II. RELATED WORK

Image mining plays a critical role in medical care. Clinical experts have unanimously agreed to improve disease detection and prevent mistakes from misinterpretation due to human errors. Priyanca et al. [1] designed a caries detection system using image processing methods such as RGB to gray conversion, gray to binary conversion, finding region of interest (ROI), background removal, division of image into same sized block and finally identification of cavities presents in X-ray image. They further claimed/demonstrated that the final identified blocks covering the cavity regions could be input to an artificial neural network with a backpropagation algorithm, and the unidentified sample could be used subsequently as a test case for caries detection. Patel et al. [2] reviewed the various enhancement, segmentation and feature extraction techniques to match the post-mortem and ante-mortem images. Huh et al. [3] proposed an automated dental cavity program for an intra oral dental X-ray imaging device which is an auxiliary diagnosis system. The system helps in early detection of caries. They further added to improve the automatic dental cavity algorithm by adding the machine learning algorithm. A case study on mostly pre molar and molar teeth was presented by Oliveira et al. to detect dental caries in panoramic dental X-ray images [4]. A feed forward artificial neural network (NN) was used for the classification. The classification accuracy of their proposed work was 98.7%. Prerna et al. proposed a comparative analysis of various segmentation techniques like edge detection, thresholding, deformable model and clustering, on the different types of dental X-ray images [5]. The comparative analysis revealed that edge detection and clustering were best suited for the periapical dental X-ray images, thresholding techniques was best suited for the bitewing dental X-ray images and deformable model was best suited for the panoramic dental X-ray images. Olsen et al. [6] employed an advanced image processing technique to detect dental caries. They used the C4.5 decision tree classifier for classification . Saravanan et al. [7] proposed a new method to detect caries using a histogram and power spectral analysis. Wang et al. [8] proposed a novel framework for automatic dental radiography analysis. Their dataset consisted of 400 cephalometric radiographs collected from 400 patient aged from 6 to 60 years. The dataset was divided into three subsets as training data, Test1 data and Test2 data. The accuracy with Test1 data was 91% and the accuracy with Test2 data is 87%. R. Manavalan et al. [9, 10] proposed a method to detect prostate cancer from transrectal ultrasound images. used Histogram, GLCM, GLRLM in order to classify the TRUS Medical Image into benign or malignant with the Support Vector Machine algorithm. Furthermore, this system was used to classify prostate cancer as benign or malignant based on the GLRLM features. The performance of the feature extraction was evaluated using parameters such as accuracy, sensitivity and specificity. The accuracy of GLCM, GLRLM and Histogram was 87%, 85% and 82% respectively. Mohanty et al. [11] proposed a method that used the extracted GLRLM features to classify the breast mass as malignant or benign, to predict early-stage cancer. They reported that the GLRLM features could be combined with other feature extraction methods, namely the LBP, GLDM (Gray Level Difference Matrix) and GLCM, to assess their joint performance for the classification of certain medical image datasets. Ozturk et al. [12] proposed the method for the classification of the histopathologic image into normal and infected using the feature extraction technique GLCM, LBP, LBGLCM, GLRLM and SFTA followed by the classification algorithm SVM, KNN and Boosted Tree Classifiers. The best accuracy was achieved with Boosted Tree algorithm using GLCM, LBP, GLRLM and SFTA as 92.8%, 89.8%, 91.8% and 94% respectively. The best accuracy using LBGLCM features was achieved with SVM as 92.9%. Dian et al. [13] proposed the method to classify the mammogram images into normal and cancerous images. The first order statistics which consists of GLCM, GLRLM and GLDM were used to extract the features. The features were used as the input to ECOC SVM classification. The result showed that GLRLM feature extraction method as the best method with 93.9% accuracy. Ozturk et al. [14] proposed a framework to classify the chest X-ray images into covid-infected and normal using the SVM (Support Vector Machine). The result showed that 78 features were extracted with the sensitivity of 83%, specificity of 96%, accuracy of 86% and precision of 86%. We have proposed a new model for the classification of the dental X-ray images into normal and infected with higher accuracy than the above mentioned techniques. High level features are more complex and have more computational load. In order to choose the best features, we have used four textural feature extraction methods LBP, GLCM, GLRLM and LBGLCM. The efficacy of these feature extraction techniques with feature reduction has been evaluated with the state of art classification algorithms for dental image classification. The main purpose of this study is to use the best feature extraction algorithm along with the PCA method to determine the most suitable features for classification of dental images with high accuracy.

III. PROPOSED WORK

The proposed work for infected Dental Image Detection System consists of five steps: Dental image pre-processing, Dental image segmentation, Feature extraction, Feature reduction and Classification (Figure 1).

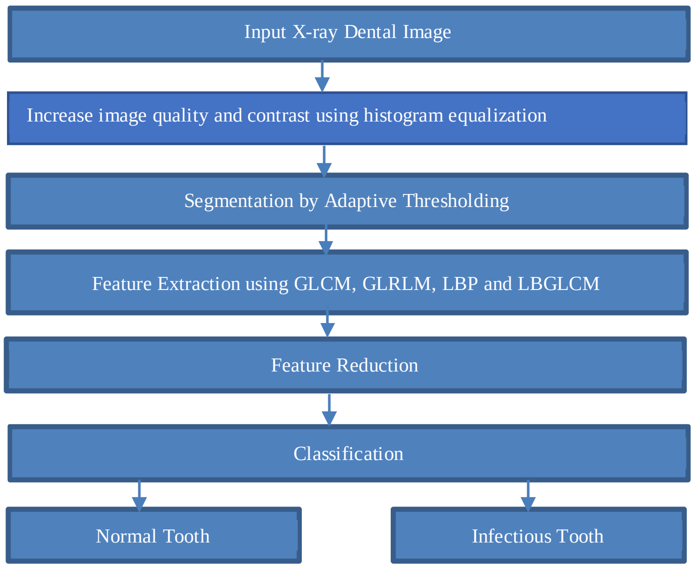

Figure 1. Dental Image Detection System

A. Dental Image Preprocessing

Contrast enhancement of the dental X-ray images enhances the accuracy of image diagnosis, thus improving the image quality and level of perception. In this study, the histogram equalization method was used to enhance the contrast of the dental X-ray images.

B. Dental Image Segmentation

The adaptive thresholding technique is routinely used in medical image processing to segment the dental X-ray images. The performance of this technique depends on the threshold value T where T is set to 127 in our implementation. This is experimentally determined based on the region of interest. The pixel value is then calculated based on the threshold. If the pixel value is less than the threshold, then the pixel is set to the back position; else, it is set to the forefront position. Figure 2 shows the dental X-ray image of the teeth. Figure 3 shows the dental image segmentation of the infected teeth by adaptive thresholding.

Figure 2. X-ray image of the teeth

Figure 3. Adaptive thresholding

C. Feature Extraction

The next step is feature extraction, which involves the identification of the vital characteristics of an image or sub-image. Textural features based on the gray-level spatial dependencies have been typically employed in image mining and classification. These textural features can be extracted from the Gray Level Co-occurrence Matrix (GLCM). Hence, in our study, we have focused on the Local Binary Pattern (LBP), Gray Level Co-occurrence Matrix (GLCM), Gray Level Run Length Matrix (GLRLM) and Local Binary Gray Level Co-occurrence Matrix (LBGLCM) for extracting textural features[12,15, 16]. These feature extraction techniques have been detailed further.

LBP: Local Binary Pattern (LBP) [17] is one of the most widely used texture pattern descriptor in the applications of image processing. LBPs compute a local representation of texture. This local representation is constructed by comparing each pixel with its surrounding neighborhood of pixels. Eq 1 and Eq 2 below are used for labeling the neighborhood pixels. The string of 0's and 1's assigned to neighbors, is converted to its decimal equivalent and assigned as the LBP code to the center pixel. The LBP feature extraction process has a window with a specified neighborhood and is traversed over the image and an LBP code is assigned to every pixel in the image (dental X-ray image in this case). The histogram features of size 2^P is extracted from the obtained LBP code.

$$LBP_{P,R} = \sum_{P=0}^{P-1} S(g_{p-}\ g_c)2^p \text{ ………. (1)}$$

$$S(x) = \begin{cases} -1, & x \geq 0 \\ 0, & x \leq 0 \end{cases} \text{ ……………… (2)}$$

where, g_c represents the central pixel gray value

g_p represents the value of the neighbors of the center pixel

P represent the number of the neighbors.

R represents the radius of the neighborhood.

GLCM: The GLCM [13] is used to extract the statistical features. The statistical features in an image can be extracted based on the distributed intensities at a specific position. The GLCM is a second order statistical feature extraction method. The regular angles used for rotation of feature extraction are 0◦, 45◦, 90◦,135◦ and there are four offsets [0,1], [-1,1], [-1,0] and [-1, -1] for four directions i.e., horizontal, vertical and two diagonals. Table I [19] specifies the list of GLCM texture features along with their formulae. P (i, j) is a second order probability function of an image region. It is of the size nXn. The (i, j)th element of the matrix represents the number of times the combination of level i and j occur in two pixels in the image when they are separated by a distance of 8 pixels along angle θ. G is number of levels specified under quantization. μ is the mean value of P, σ is the variance of the intensities, Δx, Δy is the pixel distance.

GLRLM

The GLRLM [18] is a second order statistical feature extraction method, which assigns a quantitative parameter to a gray level in the spatial domain. In the GLRLM, a texture primitive known as a gray-level run length is considered. The gray-level run length represents the maximum collinearly attached set of pixels having identical gray levels. The gray level runs are characterized by the length and direction of the run for a particular gray value. The GLRLM is able to retrieve not only the statistical information but also the structural information from the texture. Thus, it is an established efficient feature extraction method for medical images. The number of gray level runs of various lengths must be ascertained to calculate the GLRLM.

The GLRLM is calculated as $\mathrm{R}(\theta) = |\mathrm{r}'(\mathrm{i}, \mathrm{l}\theta)|$ ……………… (3)

In Eq 3, the term $\mathbf{r'(i, l\theta)}$ approximately calculates the number of times an image contains a run with length $\boldsymbol{l}$, for the gray level $\boldsymbol{i}$, in the direction of angle $\boldsymbol{\theta}$. The GLRLMs ($\boldsymbol{\theta}$) are calculated only at the defined angles of $\mathbf{0}^{\circ}$, $\mathbf{45}^{\circ}$, $\mathbf{90}^{\circ}$, and $\mathbf{135}^{\circ}$ with offset [1,2,3,4] and four direction horizontal, vertical and two diagonals. Table II presents the list of features along with their formulae. P(i, j) is defined as the image matrix in order to find the GLRLM features[18]. (i,j) represent the intensities by which pixel with gray level i is spatially related to pixel with gray level j. n denotes the total number of pixels.

LBLCM

The LBGLCM extraction method is the hybrid of LBP and GLCM. Firstly, we have applied LBP operator to the dental X-ray image and then we have applied GLCM algorithm to extract the GLCM features. Both the textural and spatial information in the image is obtained with the LBGLCM method. The features extracted from LBGLCM use the same formulae as that of GLCM. The LBGLCM algorithm provides better results than the GLCM features in dental image classification since the LBGLCM algorithm extract features by considering the

TABLE I. EXTRACTED GLCM TEXTURE FEATURES FOR DENTAL X-RAY IMAGES

FEATURES	FORMULA	FEATURES	FORMULA
Autocorrelation	$\sum_{i=0}^{G-1}\sum_{j=0}^{G-1} P(i,j)$	**Contrast**	$\sum_{n=0}^{G-1} n^2 \sum_{i=1}^{G}\sum_{J=1}^{G} P(i,j)$
Correlation	$G-1\ G-1$ $\frac{\sum_{i=0}^{G-1}\sum_{j=0}^{G-1}\{x \times j\} \times P(i,j) - \{\mu_x \times \mu_y\}}{\sigma \times \sigma}$	**Cluster prominence**	$\sum^{2G-2} (i-2\mu)^4 H_s(\Delta x,\Delta y)$
Cluster shade	$\sum (i-2\mu)^3 H_s(i\|\Delta x, \Delta y)$	**Dissimilarty**	$\sum P_{ij}\ \|i-j\|$
Energy	$\sum^{G-1}\sum^{G-1} P^2(i,j)$	**Entropy**	$-\ P(i,j) \times \log(P(i,j))$
Homogeneity	$P(i,j)(1+\|i-j\|)$	**Maximum Probability**	$\max(P_{ij})$
Sum of square	$\sum_{i=0}^{G-1}\sum_{j=0}^{G-1}(i-\mu)^2 P(i,j)$	**Sum variance**	$\sum_{i=0}^{G-1}(i-[\sum^{G-1} P_{x+y}(i)])$
Sum entropy	$-\sum_{i=0}^{2G-2} P_{x+y}(i)\log(P_{x+y}(i))$	**Difference variance**	$\sum_{i=0}^{G-1}(i-[\sum_{i=0}^{G-1} P_{x-y}(i)])^2$
Difference entropy	$\sum_{i=0}^{G-1} P_{x+y}(i)\log(P_{x+y}(i))$	**Inverse difference normalized**	$\sum_{i=0}^{G-1} \frac{P(i,j)}{1+\|i-j\|}$
Inverse difference moment	$1+(i-j)2^{P(i,j)}$	**Information measure of correlation 1**	$\sum_{i=0}^{G-1}\sum_{j=0}^{G-1} P_{ij}\ \log 2\ P_{ij}$
Angular Second Moment	$\sum_{i=0}\sum_{j=0}(P(i,j))^2$	**Sum Average**	$\sum_{i=0} iP_{x+y}(i)$

TABLE II. FEATURES DETECTED FROM GLRLM

FEATURES	FORMULA	FEATURES	FORMULA
Short-Run Emphasis (SRE)	$1/n \sum P(i,j)j^2$	**Run Percentage (RP)**	$\sum P(i,j)j$
Long-Run Emphasis (LRE)	$1/n \sum j^2 P(i,j)$	**Low Gray-level Run Emphasis (LGLRE)**	$\frac{P(i,j)}{i}$
Gray level non-uniformity (GLN)	$1/n \sum_i (\sum_j P(i,j))^2$	**High Gray-level Run Emphasis (HGLRE)**	$i^2 P(i,j)$
Run length non-uniformity (RLN)	$1/n \sum_j (\sum_i P(i,j))^2$		

using texture structure and the spatial information whereas the GLCM feature extract the information extract features based on the pixel and its neighbor.

In this paper we have used all the four feature extraction algorithms for extracting features i.e., GLCM, GLRLM, LBGLCM and LBP. The GLCM algorithm extracts a matrix with 22 image features and one class. The GLRLM algorithm extract a matrix with 7 image feature and one class. The LBP algorithm extracts a matrix with 10^6 dimension and one class and LBGLCM algorithm extract a matrix with 22 image feature and one class.

D. Feature Reduction Using PCA

Feature reduction is performed to achieve higher accuracy and better visualization of the data. Principal Component Analysis (PCA) is a form of exploratory data analysis, which is used to reduce the dimensionality of data without removing the essential features from a dataset. The application of standard PCA for feature reduction can eliminate discriminatory features, while maintaining the features that represent both groups [19, 20]. This method yields a more optimal solution as compared with the other proposed methods. Table III specifies the reduced feature set obtained after applying Principal Component Analysis to extracted features by the four feature extraction techniques.

E. Classification

The classification technique predicts the target class for each data point. We investigated various classification algorithms, such as the decision tree, random forest, decision stumps, naïve Bayes, AdaBoost, sequential minimal optimization, MLP, and radial basis function [17] to classify the dental images as normal or infected using the features extracted by LBP, GLCM, GLRLM and LBGLCM methods.

TABLE III. REDUCED FEATURES AFTER PCA

Feature Extraction Techniques	Features reduced after PCA
GLCM	ASM, Entropy, IDM, Energy, and Homogeneity.
GLRLM	RP, GLN and LGLRE
LBGLCM	Correlation, Inertia, Auto Correlation, Cluster Prominence.
LBP	10^4

IV. RESULTS AND DISCUSSION

We collected 1000 periapical dental X-ray images using the dental Radio Visio Graphy 5200 equipment, which were converted into digital images using super CMOS technology. A total of 700 dental images were used to train the algorithm, while 300 images were used for testing. The Waikato environment for knowledge analysis was used for feature reduction and image mining. MATLAB 9.2 was used for the image processing operations. The dental teeth images were preprocessed using histogram equalization to improve the quality and segmented using adaptive thresholding. Subsequently, the feature extraction process discussed earlier was used to extract the gray level texture features of the dental images using the GLCM, GLRLM, LBP and LBGLCM. The extracted features were then subjected to PCA for reduction using WEKA [21].

Performance Evaluation: The effectiveness of the classifiers used for classification was evaluated using the following parameters:

True positive rate: Defined as the true positive divided by the sum of the true positive and false positive.

False positive rate: Defined as the false positive divided by the sum of the true negative and false positive.

Accuracy: Defined as the sum of the true negative and true positive divided by the total number of samples.

Precision: Defined as the true positive divided by the sum of the true positive and false positive.

Recall: Defined as the measure of the true positive divided by the sum of true positive and false negative.

Table IV shows the performance measures of various classification techniques using the reduced textural features of the GLCM, GLRLM, LBP and LBGLCM feature extraction methods.

TABLE IV. PERFORMANCE MEASURES OF VARIOUS CLASSIFICATION TECHNIQUES USING REDUCED TEXTURAL FEATURES

	GLCM			GLRLM			LBP			LBGLCM		
	Accuracy	Precision	Recall	Accuracy	Precision	Recall	Accuracy	Precision	Recall	Accuracy	Precision	Recall
Decision Tree	87.8%	82.5%	85.7%	93.5%	93.6%	95.4%	83.4%	80.6%	84.5%	91.4%	90.6%	89.5%
Random Forest	91.5%	88.1%	89.5%	91.6%	91.3%	91.5%	85.6%	83.4%	84.7%	93.2%	91.4%	91.1%
Decision Stump	92.6%	85.3%	90.7%	94.2%	92.3%	91.4%	86.7%	81.6%	82.8%	91.3%	89.8%	92.4%
Naïve Bayes	91.9%	88.2%	89.6%	93.7%	91.6%	92.2%	88.6%	81.4%	85.4%	89.2%	88.5%	91.5%
AdaBoost	98.7%	95.9%	98.8%	95.6%	93.4%	96.5%	90.8%	88.6%	88.6%	99.7%	97.6%	94.3%
SMO	92.4%	85.3%	90.4%	90.8%	87.9%	89.4%	87.8%	85.4%	88.5%	93.3%	92.9%	94.4%
MLP	95.8%	90.4%	95.3%	97.9%	95.3%	97.4%	89.7%	87.5%	88.8%	97.6%	95.3%	93.5%
RBF	91.5%	88.6%	89.4%	93.4%	93.3%	94.5%	88.6%	84.4%	89.5%	93.5%	91.5%	90.3%

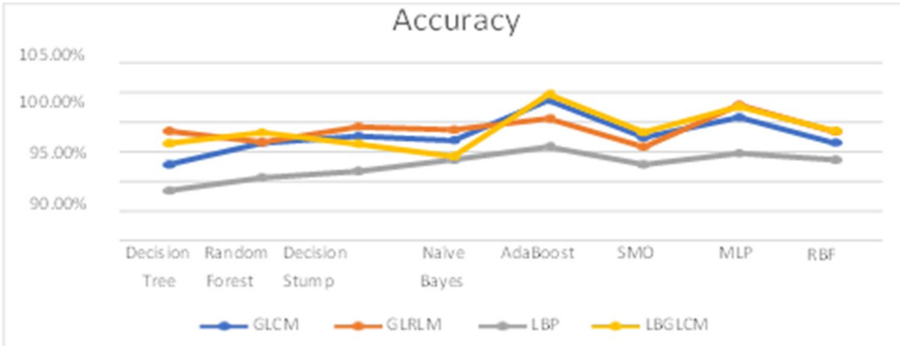

Figure 4. Accuracy values of different image mining techniques

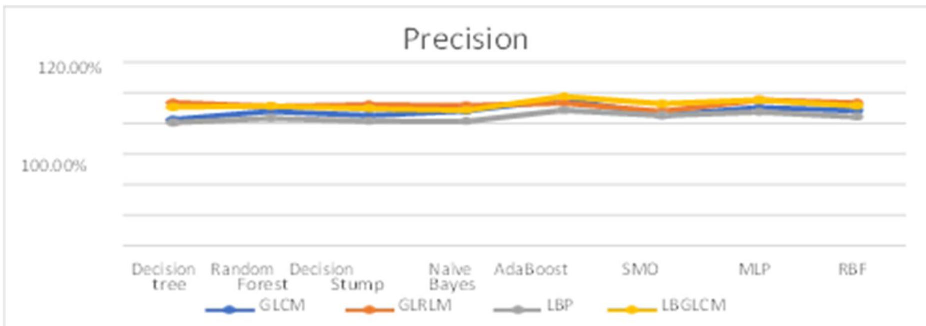

Figure 5. Precision values of different image mining techniques

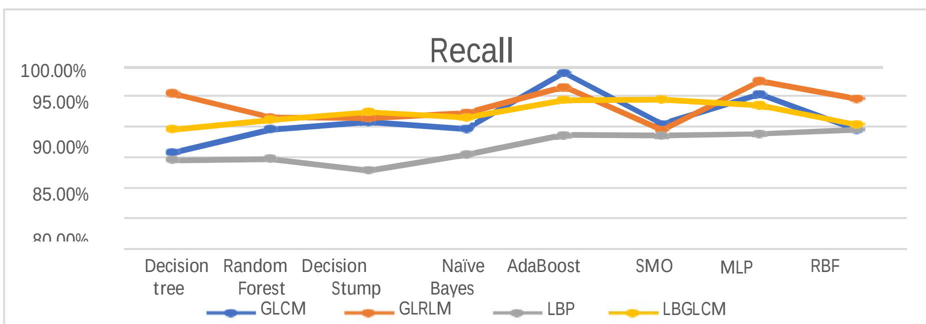

Figure 6. Recall values of different image mining techniques

The analytical bar graphs for the accuracy, precision, and recall parameters are shown in Figure 4, Figure 5, and Figure 6, respectively. With reduced GLCM, LBP and LBGLCM features, the AdaBoost classifier achieved the best accuracy, precision and recall value. With reduced GLRLM features, the MLP exhibited the highest accuracy, precision, and recall of 97.9%, 95.3%, and 97.4%, respectively. The high accuracy achieved with GLCM, GLRLM and LBGLM prove the effectiveness of these feature extraction methods in classification of dental images into normal and caries infected.

V. Conclusions

In this study, we proposed an application of image mining technique that achieved the efficient and accurate classification of dental images into normal and caries infected. The potency of the reduced feature set obtained after LBGLCM, GLCM, LBP and GLRLM feature extraction techniques for classification of dental images is shown in the achieved results. AdaBoost classifier proves to be a best classifier (accuracy 99.7%) for dental images with features extracted using LBGLCM and reduced by PCA. AdaBoost classifier also gave a high accuracy of 98.7% with GLCM feature extraction method while MLP achieved a good accuracy of 97.9% with

GLRLM method. LBP method was the least successful method that gave an accuracy of 90.8% in classifying dental images into normal and infected.

REFERENCES

[1] Priyanca P. Gonsalves, “Diagnosis of dental cavities using image processing”, International Journal of Computer Applications, vol. 180, no. 5, ISSN:0975-8887, 2017.

[2] Anita Patel, Pritesh Patel, Astha Baxi, “Analysis of Dental Image Processing for Human Identification”, International Journal of Engineering and Technology, vol. 1, issue 10, ISSN:2278-0181, 2012.

[3] Jangyong Huh, Jiman Park, Haewon Nam, Sukyoung Shin, Juhae Kim, Rena Lee, “Studies of automatic dental cavity detection system as an auxiliary tool for diagnosis of dental caries in digital X-ray image,” Progress in Medical Physics, vol. 25, pp. 52–58, 2015.

[4] Joao Oliveira, Hugo Proenca, “Caries detection in panoramic dental X-ray images,” Computational Vision and Medical Image Processing, Recent Trends Computational Methods, vol. 19, pp. 175–190, 2010.

[5] Prerna Singh, Priti Sehgal, “A comparative analysis of various segmentation techniques on dental images”, Smart and Innovative Trends in Next Generation Computing Technologies, CCIS 828, pp. 1–22, Springer, 2018.

[6] Grace F. Olsen, Susan S. Brilliant, Kayvan Najarian, David Primeaux, “An image processing enabled dental caries detection system”, ICME International Conference on Complex Medical Engineering, IEEE, ISSN:978-1-4244-3316-2, 2009.

[7] T. P. Saravanan, M. Sundar Raj, Kannaki Gopalakrishnan, “Identification of early caries in human tooth using histogram and power spectral analysis”, Middle-East Journal of Scientific Research, vol. 7, pp. 871–875, 2014.

[8] Ching-Wei Wang, Cheng-Ta Huang, Jia-Hong Lee, Chung-Hsing Li, Sheng-Wei Chang, Ming-Jhih Siao, Tat-Ming Lai, Bulat Ibragimov, Tomaž Vrtovec, Olaf Ronneberger, Philipp Fischer, Tim F. Cootes, Claudia Lindner, "A benchmark for comparison of dental radiography analysis algorithms", Medical Image Analysis, vol. 31, Pages 63-76, ISSN 1361-8415, 2016.

[9] Manavalan Radhakrishnan,Thangavel Kuttiannan, “Comparative Analysis of Feature Extraction for the Classification of Prostate Cancer from TRUS Medical Images”, International Journal of Computer Science Issues, vol. 9, issue 1, no. 2, 2012, ISSN 1694-0814.

[10] [17] R. Manavalan, K. Thangavel, “Evaluation of textural features extraction from GLRLM for prostate cancer TRUS medical images”, International Journal of Advances in Engineering & Technology, vol. 2, issue 1, pp. 401–409, 2012.

[11] Aswini Kumar Mohanty, Swapnasikta Beberta, Saroj Kumar Lenka, “Classifying benign and malignant mass using GLCM and GLRLM based texture features from mammogram”, International Journal of Engineering Research and Applications, vol. 1, issue 3, pp. 687– 693, 2011.

[12] Saban Ozturk, Bayram Akdemir, “Application of Feature Extraction and Classification Methods for Histopathological Image using GLCM, LBP, LBGLCM, GLRLM and SFTA”, International Conference on Computational Intelligence and Data Science (ICCIDS 2018), Procedia Computer Science, vol. 132, pp. 40-46, 2018.

[13] Novitasari, Dian & Lubab, Ahmad & Sawiji, Asri & Asyhar, Ahmad, “Application of Feature Extraction for Breast Cancer using One Order Statistic, GLCM, GLRLM, and GLDM”, Advances in Science, Technology and Engineering Systems Journal, issue 4, 10.25046/aj040413, 2019.

[14] Saban Ozturk, Umut Ozkaya and Mucahid Barstuyan, “Classification of Coronavirus (Covid-19) from X-ray and CT images using shrunken features”, International Journal of Imaging and System Technology, 2020.

[15] Madasamy Sornam and M. Prabhakaran, “Logit-based artificial bee colony optimization approach for dental caries classification using a back propagation neural network”, Integrated Intelligent Computing, Communication, and Security, Studies in Computation Intelligence, Springer, ISSN:978-981-10-8797-4, 2019.

[16] Ivan Kitanovski, Katarina. Trojacanec, Ivica Dimitrovski, Suzana Loskovska, “Modality classification using texture features”, ICT Innovations, vol. 150, Advances in Intelligent and Soft Computing, pp. 189–198, 2011.

[17] Di Huang,Caifeng Shan,Mohsen Ardabilian,Liming Chen,Yunhong Wang, “Local Binary Patterns and its application to Facial Image Analysis: A survey”, IEEE Transaction on Systems Man and Cybernetics, vol. 41, issue 6, pp. 765-781.

[18] Prerna Singh, Priti Sehgal, “Automated caries detection based on radon transformation of DCT”, 8^{th} International Conference on Computing, Communication, and Networking (ICCCNT), pp.1-6, 2017.

[19] Shruti Sehgal, Harpreet Singh, Mohit Agarwal, V. Bhaskar, Shantanu, “Data analysis using principal component analysis”, International Conference on Medical Imaging, m-Health and Emerging Communication Systems (MedCom), IEEE, pp. 45–48, 2014.

[20] Young-Suk Shin, Myung Su Kim, “Human identification system based on PCA using geometric feature of teeth”, International Conference on Biometrics, Advances in Biometrics, Lecture Notes of Computer Science, vol. 3832, pp. 751–755, 2006

[21] http://www.cs.waikato.ac.nz/ml/weka/